In Computational Plasticity: Fundamentals and Applications, D.R.J. Owen, E. Oñate, and E. Hinton, eds., Pineridge Press, 1341-1348, 1997.

Algorithm for Optimization of Steady Forming Processes

Antoinette M. Maniatty[1] and Ming-Fa Chen[2]

[1]Department of Mechanical Engineering, Aeronautical Engineering and Mechanics
Rensselaer Polytechnic Institute
Troy, New York 12180, U.S.A.

[2]China Steel Corporation
Kaohsiung 81233 Taiwan, R.O.C.

Abstract. This work presents a numerical optimization algorithm for designing steady forming processes. The design problem considered involves producing a specified material property distribution in formed materials where the forming process can be approximated as steady. The design parameters are the process geometry and, in some cases, the speed. The material property of interest is a scalar internal variable which is meant to represent the state of the material. The tool shape optimization described in this study is the nonlinear inverse problem that determines the two-dimensional forming geometry used to satisfy a specified design criterion which is to generate a desired material property distribution in the final product. In this work, an objective function is combined with a penalty function to form an unconstrained function to be minimized. The BFGS (Broyden-Fletcher-Goldfarb-Shanno) quasi-Newton method with a Brent method line search is used to perform the minimization. Details of the algorithm and update procedures as well as results for extrusion and rolling processes are presented.

1 INTRODUCTION

In forming processes, the material characteristics of the products are sensitive to the process parameters. These process parameters generally include geometry, temperature, speed of both the tool and the workpiece, etc. The process designer must carefully choose these parameters in order to produce the desired products at a low cost. This is a process design problem. Most studies in recent years formulate this design problem as a series of direct problems. A direct problem is mathematically based on a set of input information, including the domain, governing equations, constitutive relations, and boundary conditions. After this information is provided, a solution for the deformation, stress and internal state variable fields through the deformation zone is calculated. In the forward solution procedure, different design parameters are tried and the direct problem is solved repeatedly until a satisfactory design is reached.

In fact, a solution formulation for such design problems should start with the product specifications as input, and then compute the process design parameters which will generated the desired product. This formulation for a design problem in forming is effectively the inverse of the forward or direct problem formulation. Hence, this class of problems is termed inverse problems. In inverse problems, unknown boundary conditions or parameters are determined based on given data regarding the solution (or desired solution).

This work focuses on developing a design tool to determine the optimal process parameters for steady forming operations. For example, the process parameters may define the tool shape. This design problem is usually referred to as shape optimization. Particularly, the tool shape optimization described in this study is the nonlinear inverse problem that determines the two-dimensional forming geometry that satisfies the design criterion of generating a desired material property distribution in the final product. The material property of interest is defined as an internal state variable.

In the process design problem considered herein, an unconstrained function is formulated to be minimized. This function consists of an objective function and a penalty function. The objective function represents the deviation between the specified and simulated internal state variables. The penalty function is added to apply additional constraints. The BFGS (Broyden-Fletcher-Goldfarb-Shanno) quasi-Newton method [1] combined with a Brent method [2] line search is chosen for function minimization in this study because this method was found to be superior for efficiency and accuracy. Design sensitivities are necessary for the minimization algorithm. An explicit matrix formulation of sensitivities using the adjoint method is used for this purpose [3].

2 DIRECT FORMULATION

The formulation for the direct metal forming problem follows that given in Dawson [4]. Summarizing, consider a two dimensional domain B with boundary ∂B where the material being deformed is flowing steadily through the domain. The boundary value problem for equilibrium on B is regarded as a control volume problem and is expressed in the following equations:

$$div\,\mathbf{T} = \mathbf{0} \qquad \text{on } B \tag{1}$$

$$\mathbf{e}_i \cdot \mathbf{u} = \hat{u}_i \qquad \text{on } \partial B_{1i} \tag{2}$$

$$\mathbf{e}_i \cdot (\mathbf{Tn}) = \hat{t}_i \qquad \text{on } \partial B_{2i} \tag{3}$$

$$\mathbf{e}_i \cdot (\mathbf{Tn}) = \beta(u_{oi} - u_i) \qquad \text{on } \partial B_{3i} \tag{4}$$

where $\mathbf{T}$ is the Cauchy stress tensor, $\mathbf{u}$ is the velocity vector, $\hat{u}_i$ is the velocity specified on ∂B_{1i}, $\hat{t}_i$ is the traction specified on ∂B_{2i}, $\mathbf{n}$ is the unit outward normal vector on ∂B, and $\mathbf{e}_i$ form an orthonormal basis for the two-dimensional space with i = 1,2. The fourth equation represents a hydrodynamic friction law where u_{0i} is the tangential velocity of the tool on ∂B_{3i} and β is the coefficient of hydrodynamic friction which is taken as constant for simplicity in this analysis. The boundary conditions must be specified on the entire boundary for each degree of freedom without overlap.

The material behavior is assumed be isochoric, and elasticity is neglected for simplicity. This is reasonable for large deformation metal plasticity as long as springback and residual stresses are not a concern, as is the case in this analysis. The constitutive equations can be summarized as

$$tr(\mathbf{D}) = div\,\mathbf{u} = \mathbf{0} \tag{5}$$

$$\dot{\tilde{\varepsilon}} = f(\tilde{\sigma}, s) \tag{6}$$

$$\mathbf{T}' = \frac{2\tilde{\sigma}}{3\dot{\tilde{\varepsilon}}}\mathbf{D} \tag{7}$$

$$\dot{s} = \nabla s \cdot \mathbf{u} = g(\dot{\tilde{\varepsilon}}, s) \tag{8}$$

$$s = \hat{s} \quad \text{on } \partial B_s \tag{9}$$

where $\mathbf{D}$ is the rate of deformation tensor, $\dot{\tilde{\varepsilon}}$ and $\tilde{\sigma}$ are the von Mises effective strain rate ($\dot{\tilde{\varepsilon}} = \sqrt{\frac{2}{3}\mathbf{D}\cdot\mathbf{D}}$) and stress, respectively, s is a scalar internal variable, and $\mathbf{T}'$ is the deviatoric Cauchy stress tensor. The middle term in equation (8) results from the assumption of steady state material flow. Equation (9) is a boundary condition defining the state variable field on the boundary ∂B_s where the material enters the domain of interest. Equations (1) - (7) are discretized by expressing the velocity, state variable, and hydrostatic pressure fields in terms of finite element interpolation functions and using the consistent penalty method [5] to enforce incompressibility. In addition, allowing for a discontinuous pressure field so that pressures can be eliminated easily from the system of equations, the system is reduced to a nonlinear system of equations of the matrix form

$$\underline{\mathbf{k}}(\underline{\mathbf{u}}, \underline{\mathbf{s}}) = \underline{\mathbf{f}} \tag{10}$$

where $\underline{\mathbf{u}}$ and $\underline{\mathbf{s}}$ are vectors of the nodal velocities and state variables, respectively, and $\underline{\mathbf{f}}$ is the force vector. Equation (8) subject to condition (9) can also be discretized to provide a second nonlinear system of matrix equations of the form

$$\underline{\mathbf{h}}(\underline{\mathbf{u}}, \underline{\mathbf{s}}) = \underline{\mathbf{0}} \tag{11}$$

where it should be noted that since equation (8) is a convection equation, a streamline upwind method [6] is needed to stabilize equation (11). A staggered procedure is used to solved the coupled system of nonlinear equations defined in (10) and (11)

for the nodal velocities $\underline{\mathbf{u}}$ and the nodal state variables $\underline{\mathbf{s}}$. For details see [3].

3 INVERSE PROBLEM DEFINITION

In this case, the same governing equations and boundary conditions are prescribed, but now part of the shape of the boundary $\partial\hat{B}$, which represents the process geometry, and possibly also the driving process velocity (either specified by a velocity or friction boundary condition) are not known. The shape can be parameterized by a position vector $\hat{\mathbf{x}}(\xi)$ which can be parameterized by

$$\mathbf{e}_i \cdot \hat{\mathbf{x}}(\xi) = b_{i\alpha}\varphi_\alpha(\xi) \quad \hat{\mathbf{x}} \in \partial\hat{B} \qquad (12)$$

where $b_{i\alpha}$ (or $\underline{\mathbf{b}}$ in direct notation) are the shape design parameters, φ_α are the shape functions where subscript $\alpha = 1, N_{\hat{B}}$ represents the discrete points used to parameterize the boundary $\partial\hat{B}$, and ξ is a measure of distance along $\partial\hat{B}$. Let u_d be the unknown driving velocity. Now the nonlinear system of equations (10) and (11) becomes

$$\underline{\mathbf{k}}(\underline{\mathbf{u}},\underline{\mathbf{s}},\underline{\mathbf{b}},u_d) = \underline{\mathbf{f}}(\underline{\mathbf{b}},u_d) \qquad (13)$$

$$\underline{\mathbf{h}}(\underline{\mathbf{u}},\underline{\mathbf{s}},\underline{\mathbf{b}}) = \underline{\mathbf{0}} \qquad (14)$$

where $\underline{\mathbf{b}}$ and u_d are added to the list of solution variables to be determined.

The goal now is to find the design parameters $\underline{\mathbf{b}}$ and u_d which satisfy equations (13) and (14) and minimize the following objective function

$$\Lambda = \left(\underline{\mathbf{s}}^* - \hat{\underline{\mathbf{s}}}^*\right)^T \left(\underline{\mathbf{s}}^* - \hat{\underline{\mathbf{s}}}^*\right) + \Omega \qquad (15)$$

where $\underline{\mathbf{s}}^*$ is the vector of model nodal state variables at discrete locations in the exit region of the process geometry on ∂B_e, $\hat{\underline{\mathbf{s}}}^*$ is the corresponding vector of desired state variables, and Ω is a constraint term. The constraints on the solution variables can be generally expressed as a set of inequality constraints

$$G_i(\underline{\mathbf{b}},u_d) \le 0, \quad i = 1,N_c \qquad (16)$$

where N_c represents the number of constraints. For example, if discretized position coordinates are the design variables, a constraint may be such that a specific coordinate cannot be greater than or less than some specified value. There are numerous methods for defining constraint terms in a functional form to enforce inequality constraints [7,8]. In this work, Ω is defined by the following function

$$\Omega = \frac{1}{2}\sum_{i=1}^{N_c} \lambda_i^c \left\langle G_i(\underline{\mathbf{b}},u_d) + \omega_i \right\rangle^2 + \hat{c}\left\langle G_i(\underline{\mathbf{b}},u_d) + \hat{\eta}\right\rangle\left\langle \lambda_i^c - \hat{\lambda}^c \right\rangle \qquad (17)$$

where λ_i^c and ω_i are penalty parameters and Lagrange multipliers for each constraint which need to be updated in the minimization procedure. The angle brackets $\langle\cdot\rangle$ denote a singularity function. The other parameters, $\hat{c}$, $\hat{\eta}$, and $\hat{\lambda}^c$, remain fixed.

4 MINIMIZATION ALGORITHM

The BFGS method [1] combined with a Brent method [2] line search was found to be effective in minimizing the highly nonlinear system of equations defined in the previous section. The minimization algorithm proceeds as follows:

(1) Make an initial guess for the design parameters $\underline{\mathbf{b}}^{(0)}$ and $u_d{}^{(0)}$. Initialized the penalty parameters $\lambda_i^{c(0)}$ and Lagrange multipliers $\omega_i{}^{(0)}$. Set the iteration number $r = 0$.

(2) Solve the direct problem for the corresponding velocity $\underline{\mathbf{u}}^{(r)}$ and state variable fields $\underline{\mathbf{s}}^{(r)}$.

(3) Compute the objective function $\Lambda^{(r)}$ as defined in equations (15) and (17).

(4) Compute the gradient of the objective function

$$\underline{\mathbf{g}}^{(r)} = \frac{d\Lambda^{(r)}}{d\underline{\mathbf{q}}} = \underline{\mathbf{C}}^{(r)T}\left(\underline{\mathbf{s}}^{*(r)} - \hat{\underline{\mathbf{s}}}^*\right) + \sum_{i=1}^{N_c} \lambda_i^c \left\langle G_i^{(r)} + \omega_i \right\rangle \frac{dG_i{}^{(r)}}{d\underline{\mathbf{q}}} \qquad (18)$$

where $\underline{\mathbf{q}}^{(r)} = (\underline{\mathbf{b}}^{(r)}, u_d{}^{(r)})$ and $\underline{\mathbf{C}}^{(r)} = \frac{d\underline{\mathbf{s}}^{*(r)}}{d\underline{\mathbf{q}}}$ is the matrix of design sensitivities. For details on the calculation of the design sensitivity matrix see [3].

(5) Check for convergence using the following criteria

$$\Lambda^{(r)} \le \varepsilon_1$$

$$\left|\Lambda^{(r)} - \Lambda^{(r-1)}\right| \le \varepsilon_2 \Lambda^{(r)}$$

$$\sqrt{\underline{\mathbf{g}}^{(r)^T} \underline{\mathbf{g}}^{(r)}} \le \varepsilon_3$$

If all the convergence criteria are met, then the algorithm is finished, otherwise, continue.

(6) Compute the search direction, $\underline{\mathbf{d}}^{(r)}$, using the BFGS approximation for the inverse Hessian of the objective function, $\underline{\mathbf{H}}^{(r)}$. The initial value for $\underline{\mathbf{H}}^{(0)}$ is the identity matrix.

$$\underline{\mathbf{d}}^{(r)} = -\underline{\mathbf{H}}^{(r+1)} \underline{\mathbf{g}}^{(r)} \tag{19}$$

(7) Update the vector of design parameters using a line search.

$$\underline{\mathbf{q}}^{(r+1)} = \underline{\mathbf{q}}^{(r)} + \alpha \underline{\mathbf{d}}^{(r)} \tag{20}$$

The details of how to find α are given in an algorithm described in section 4.1.

(8) Compute the constraint function $\Omega^{(r)}$ and test for a constraint violation. If a constraint violation exists, update the Lagrange multipliers and penalty parameters using the algorithm defined in section 4.2 and go back to step (3), otherwise continue.

(9) The matrix $\underline{\mathbf{H}}^{(r)}$ is updated for future iterations using the formula

$$\underline{\mathbf{H}}^{(r+1)} = \underline{\mathbf{H}}^{(r)}$$

$$+\left(1 + \frac{\underline{\mathbf{w}}^{(r)^T} \underline{\mathbf{H}}^{(r)} \underline{\mathbf{w}}^{(r)}}{\underline{\mathbf{v}}^{(r)^T} \underline{\mathbf{w}}^{(r)}}\right) \frac{\underline{\mathbf{v}}^{(r)} \underline{\mathbf{v}}^{(r)^T}}{\underline{\mathbf{v}}^{(r)^T} \underline{\mathbf{w}}^{(r)}}$$

$$-\left(\frac{\underline{\mathbf{v}}^{(r)} \underline{\mathbf{w}}^{(r)^T} \underline{\mathbf{H}}^{(r)} + \underline{\mathbf{H}}^{(r)} \underline{\mathbf{w}}^{(r)} \underline{\mathbf{v}}^{(r)^T}}{\underline{\mathbf{v}}^{(r)^T} \underline{\mathbf{w}}^{(r)}}\right) \tag{21}$$

where

$$\underline{\mathbf{v}}^{(r)} = \underline{\mathbf{q}}^{(r+1)} - \underline{\mathbf{q}}^{(r)}$$

$$\underline{\mathbf{w}}^{(r)} = \underline{\mathbf{g}}^{(r+1)} - \underline{\mathbf{g}}^{(r)}$$

Go to step (2) and continue.

4.1 Line search

Brent's method [2] is used for performing the line search in step (7) of the preceding algorithm. An outline of this algorithm is as follows:

(1) Determine the bracketing interval $\alpha \subset [\alpha_l, \alpha_u]$. The initial lower bound point is $\alpha_l = 0$ (this gives back the solution from the previous iteration in equation (20)). The initial upper bound point is given based on the upper and lower geometric bound constraints. This is computed by

$$\alpha_u = \min(\alpha_i'), \qquad i = 1, N_c$$

$$\alpha_i' = \max(\alpha_i^l, \alpha_i^u), \qquad i = 1, N_c$$

where

$$\alpha_i^l = \frac{b^l - b_i^{(r)}}{d_i^{(r)}}, \quad \alpha_i^u = \frac{b^u - b_i^{(r)}}{d_i^{(r)}}$$

b_l and b_u are the upper and lower bounds of the design parameters, and the subscript i symbolically means the value at the corresponding geometric location for a given constraint.

(2) Initialize intermediate function points $\alpha_1 = \alpha_2 = \alpha_3 = \alpha_u$.

(3) Check for convergence on the interval size. If

$$\Delta_\alpha = \frac{\alpha_1 - \alpha_l}{\alpha_1} \le \varepsilon_\alpha$$

Then converged and take $\alpha = \alpha_1$ for use in equation (20), otherwise, continue.

(4) If this is not the first iteration, evaluate two trial points, α^*, by the secant method.

$$\alpha^* = \frac{\alpha_j \Lambda'(\alpha_j) - \alpha_1 \Lambda'(\alpha_1)}{\Lambda'(\alpha_j) - \Lambda'(\alpha_1)} - \frac{2\left[\Lambda(\alpha_j) - \Lambda(\alpha_1)\right]}{\Lambda'(\alpha_j) - \Lambda'(\alpha_1)} \quad (22)$$

where $\Lambda'(\alpha_i) = \underline{\mathbf{g}}(\alpha_i)^T \underline{\mathbf{d}}(\alpha_i)$, and where j = 2, 3. An acceptable trial point must satisfy the two criteria (i) it must be in the descent direction measured from α_1 and (ii) it must be in the interval $[\alpha_l, \alpha_u]$. If both trial points are acceptable, choose the one closest to α_l. If neither point is acceptable, or if this is the first iteration, go to step (5), otherwise go to step (6).

(5) Determine the trial point by the bisection method

$$\alpha^* = \frac{\alpha_1 + \alpha_k}{2} \quad (23)$$

where $k = u$ if $\Lambda'(\alpha_1) < 0$, otherwise $k = l$.

(6) If $\Lambda(\alpha^*) > \Lambda(\alpha_1)$, and $\Delta_\alpha < 10^2 \varepsilon_\alpha$, then let the trial point be determined by parabolic interpolation

$$\alpha^* = \alpha_1 + \frac{1}{2}\frac{f^2 g - h^2 k}{fg - hk} \quad (24)$$

where $f = \alpha_2 - \alpha_1$, $g = \Lambda(\alpha_3) - \Lambda(\alpha_1)$, $h = \alpha_3 - \alpha_1$, and $k = \Lambda(\alpha_2) - \Lambda(\alpha_1)$.

(7) The bracket bounds are updated according to

(a) if $\Lambda(\alpha^*) > \Lambda(\alpha_1)$, then

$\alpha_u = \alpha^*$, if $\alpha_1 \le \alpha^*$ or

$\alpha_l = \alpha^*$, if $\alpha_1 > \alpha^*$

(b) if $\Lambda(\alpha^*) \le \Lambda(\alpha_1)$, then

$\alpha_u = \alpha_1$, if $\alpha_1 \le \alpha^*$ or

$\alpha_l = \alpha_1$, if $\alpha_1 > \alpha^*$.

(8) The parameters α_1, α_2, and α_3 are redefined as the points where the three smallest function evaluations so far are at so that $\Lambda(\alpha_1) \le \Lambda(\alpha_2) \le \Lambda(\alpha_3)$. Return to step (3).

4.2 Constraint parameter update

The following algorithm is used to update the Lagrange multipliers, λ_i^c, and penalty parameters, ω_i.

(1) Let r' be the iteration number for the constraint update procedure; r' is set to zero at the beginning of the minimization procedure. The following parameters are initialized at the beginning of the minimization procedure: $\lambda_i^{c(0)}$, $\omega_i^{(0)}$, $\hat{e}^{(0)}$, a, $\bar{a}$, c, and $\hat{\eta}$. Also $\hat{c}$ is initialized to zero, and $\hat{\lambda}^c$ is defined as $\hat{\lambda}^c = 10^9 \Lambda^{(0)}$.

(2) Compute the parameter $e^{(r')}$ using:

$$\bar{e}_i^{(r')} = max\left(G_i, -\omega_i^{(r')}\right), \; i = 1, N_c \quad (25)$$

$$e^{(r')} = max\left(\left|\bar{e}_i^{(r')}\right|\right), \quad i = 1, N_c \quad (26)$$

(3) If $e^{(r')} < \hat{e}^{(r')}$, then update the Lagrange multipliers

$$\omega_i^{(r'+1)} = \omega_i^{(r')} + \bar{e}_i^{(r')} \quad (27a)$$

otherwise

$$\omega_i^{(r'+1)} = \omega_i^{(r')} \quad (27b)$$

(4) If $e^{(r')} < \frac{\hat{e}^{(r')}}{a}$, then go to step (6). Otherwise, check each constraint, i = 1, N_c. If $\left|\bar{e}_i^{(r')}\right| > \frac{\hat{e}^{(r')}}{a}$, then update the penalty parameters and the Lagrange multipliers for constraint i.

$$\lambda_i^{c(r'+1)} = c\lambda_i^{c(r')} \quad (28)$$

$$\omega_i^{(r'+1)} = \frac{\omega_i^{(r'+1)}}{c} \quad (29)$$

(5) If an ill-condition appears, i.e. if the geometric constraint violations cannot be improved by the algorithm as it is progressing, then set $\hat{c}$ equal to a big number. Now the second term in equation (17) becomes effective and helps to reduce the ill-condition. Go to step (7).

(6) Update $\hat{e}$,

$$\hat{e}^{(r'+1)} = \bar{a}e^{(r')} \tag{30}$$

(7) Exit the update routine.

5 NUMERICAL RESULTS

The design of round-to-round extrusion and flat rolling processes are presented to demonstrate the stability and convergence of the numerical algorithm for the nonlinear inverse problem of interest. These examples involve the problem of determining the optimum die geometry for extrusion and the optimum speed and process geometry for rolling to generate the state variable distribution as close as possible to the specified distribution. The examples focus on demonstrating the ill-posedness or well-posedness of these problems.

The geometry and the design parameters of the design forming problems considered herein are shown in Figure 1, where $\partial\tilde{B} = \partial B_{1y} + \partial B_{2x}$ represents a surface with a symmetric boundary conditions, $\partial B' = \partial B_{1x} + \partial B_{2y}$ represents a surface with a prescribed driving velocity in extrusion, $\partial B^f = \partial B_{2x} + \partial B_{2y}$ represents a free surface, and $\partial\hat{B} = \partial B_{3x'} + \partial B_{1y'}$ represents surface with a friction boundary condition which is also the surface with the tool shape to be optimized. The coordinates x' and y' are tangent and normal coordinates on $\partial\hat{B}$, respectively. The material in these examples is taken to be 1100 aluminum at 450°C. The viscoplastic model given in Brown et al. [9] is used. The friction coefficient β is taken to be 0.1 and 1.0 GPa s m^{-1} for light, and high friction, respectively, and the penalty parameter for imposing incompressibility is 10^{11}. The parameters initialized for the constraint term are $\omega_i^{(0)} = 0$, $\lambda_i^{c(0)} = 10^{-6}$, $\hat{e}^{(0)} = 10^8$, $a = 4$, $\bar{a} = 1$, $c = 100$, and, $\hat{\eta} = 2\times10^{-5}$. In general, these parameters are problem dependent, and numerical experiments need to be carried out, perhaps first on a coarse mesh, to test what these parameters should be, in order to accelerate convergence.

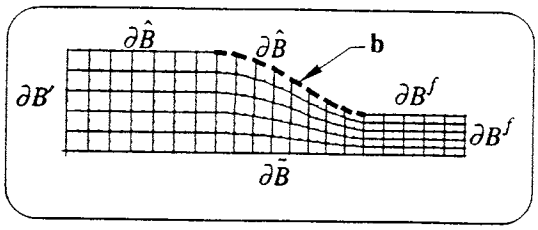

Figure 1(a): Extrusion geometry.

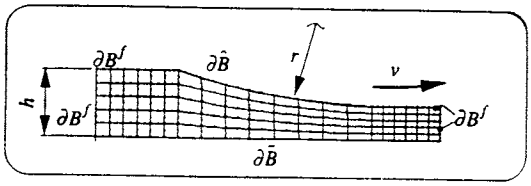

Figure 1(b): Rolling geometry

First consider the round-to-round extrusion problem. The reduction and the length of the die is assumed constant in the design. A light friction is considered in the extrusion process. The die profile does not have any constraint other than the die must be converging, i.e. from left-to-right, the die must always be getting smaller, never larger. Four initial die profiles were used as initial guesses to start the minimization procedure. Two optimal die profiles were found (Figure 2) which generate the exact uniform distribution of the state variable at 45 MPa which was specified to the tolerance of $O(10^{-11})$. The solution to this problem is therefore non-unique, and the solution depends on the initial guess. In this case, the initial die profile converges to the optimal die profile which is closest to it. The state variable distributions for those die profiles are shown in Figure 3.

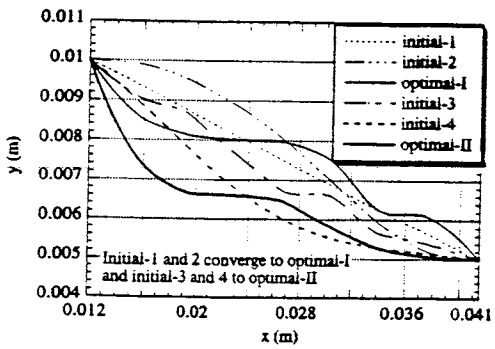

Figure 2: Two optimal extrusion die profiles

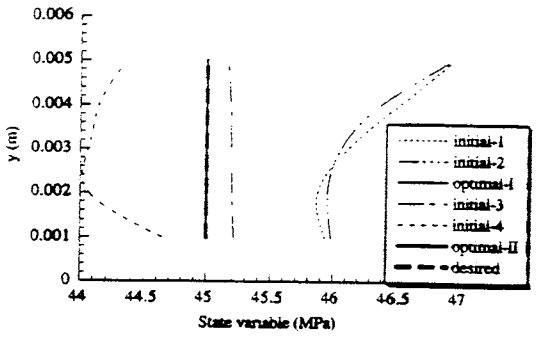

Figure 3: State variable distributions for extrusion profiles

The design variables for the flat rolling problem are roll radius, reduction, and rolling speed. High friction is considered. In the first case, the desired state variable field is taken to be a constant 45 MPa. For this rolling problem, the optimum roll radius is 6.11 cm, reduction 39.02%, and rolling speed 7.70 cm/sec. The rolling process with these parameters produces the most uniform distribution at 45 MPa for the state variable as shown in Figure 4. In the second case, a linearly varying state variable field was specified as the desired state variable field. For this distribution, the optimal roll radius is 2.24 cm, reduction is 72.22%, and rolling speed is 19.94 cm/sec. The resulting state variable field is shown in Figure 5.

6 CONCLUSIONS

Solution procedures and numerical algorithms for determining optimum process parameters in steady forming processes have been presented. The process design problems examined involve determining the process parameters that generate a desired internal state variable field in the final product. Examples involving extrusion and rolling were used to demonstrate the effect of the process parameters on the resulting state variable field, and to demonstrate the inverse algorithm. The solution procedure has been found to give convergent solutions for the nonlinear inverse problems investigated, however, the solution may not be unique, or may not be close enough to the desired state variable field to be considered acceptable.

ACKNOWLEDGMENTS

This work was supported by the Henry Luce Foundation, Inc. and by the National Science Foundation through Grant DMI-9358123.

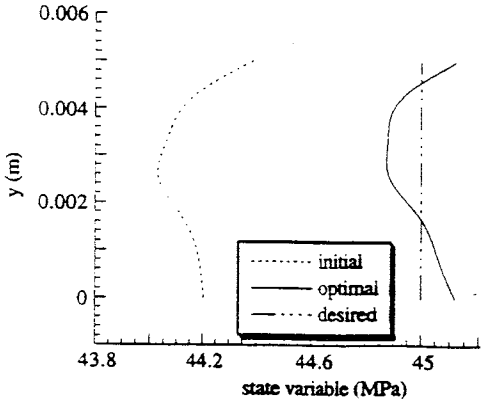

Figure 4: State variable distribution for rolling case 1

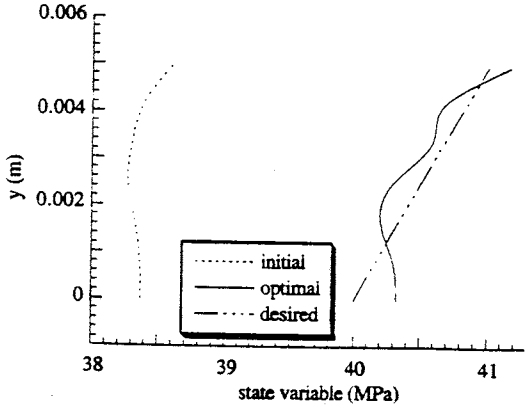

Figure 5: State variable distribution for rolling case 2

REFERENCES

[1] R. Fletcher, *Practical Methods of Optimization*, John Wiley and Sons, Ltd., New York, 1987.

[2] R. P. Brent, *Algorithms for Minimization without Derivatives*, Prentice-Hall, New Jersey, 1973.

[3] A. M. Maniatty and M.-F. Chen, "Shape sensitivity analysis for steady metal-forming processes," *Int. J. Numer. Methods Engng.* **39**, 1199-1217, 1996.

[4] P. R. Dawson, "On modeling of mechanical property changes during flat rolling of aluminum," *Int. J. Solids Struct.* **23**, 947-968, 1987.

[5] M. S. Engelman, R. L. Sani, P. M. Gresho, and M. Bercovier, "Consistent versus reduced integration penalty methods for incompressible media using several old and new elements", *Int. J. Numer. Meth. Fluids* **2**, 25-42, 1982.

[6] T. J. R. Hughes and A. N. Brooks, "A theoretical framework for Petrov-Galerkin methods with discontinuous weighting

functions," in *Finite Elements in Fluids* (eds. R. H. Gallagher et al.), vol. 4, 47-65, Wiley, Chichester, 1982.

[7] M. J. D. Powell, "A method for nonlinear constraints in minimization problems", in R. Fletcher Ed., *Optimization*, Academic Press, New York, 1969.

[8] J. S. Arora, A. I. Chahande, and J. K. Paeng, "Multiplier methods for engineering optimization", *Int. J. for Numerical Methods in Engng.* **32**, 1485-1525, 1991.

[9] S. B. Brown, K. H. Kim and L. Anand, "An internal variable constitutive model for hot working of metals", *Int. J. Plasticity* **5**, 95-130, 1989.